JOURNAL OF VIROLOGY, Sept. 1995, p. 5716–5722 Vol. 69, No. 9
0022-538X/95/$04.00+0

Nucleocapsid Protein Effects on the Specificity of Retrovirus RNA Encapsidation

YAQIANG ZHANG AND ERIC BARKLIS*

Vollum Institute for Advanced Biomedical Research and Department of Molecular Microbiology and Immunology, Oregon Health Sciences University, Portland, Oregon 97201-3098

Received 1 March 1995/Accepted 13 June 1995

We have analyzed the roles of Gag protein nucleocapsid (NC) domains in the packaging or encapsidation of retroviral RNAs into virus particles. We found that mutation of both zinc finger motifs of the human immunodeficiency virus (HIV) NC domain reduced but did not eliminate encapsidation of the HIV viral RNA. However, the NC mutations also resulted in a three- to fourfold reduction in the specificity of RNA encapsidation, as determined by comparison of virus-associated genomic and spliced RNA levels. As a complementary approach, we replaced the NC domain of Moloney murine leukemia virus (M-MuLV) with that of HIV. Chimeric virus particles assembled efficiently, were of wild-type M-MuLV density, and cross-linked at NC cysteines. In encapsidation studies, wild-type M-MuLV precursor Gag (Pr^{Gag}) proteins packaged M-MuLV transcripts more efficiently than HIV RNAs. In contrast, chimeric Pr^{Gag} proteins possessing the HIV-1 NC domain in the context of the M-MuLV MA (matrix), p12, and CA (capsid) domains encapsidated HIV transcripts to a greater extent than M-MuLV transcripts. Our results support the notion that retroviral NC domains contribute toward both the efficiency and specificity of viral genomic RNA packaging.

Retrovirus particles contain a genomic complement of two molecules of viral genomic RNA, but a provirus also may give rise to a variety of smaller, singly or multiply spliced subgenomic mRNAs. Although viral spliced RNAs and cellular RNAs may be packaged into virus particles, the packaging of viral genomic RNA is essential for the newly formed virus to be infectious. Thus, the encapsidation of retroviral genomes must be selective enough to overcome the high background of cellular RNAs and subgenomic viral RNAs. Two components are involved in specific encapsidation of viral genomic RNA: the secondary and tertiary structures of genomic viral RNA and the Gag or Gag-Pol proteins which form assembling virus particles. The specificity with which retroviral full-length genomic RNAs are encapsidated suggests that specific sequences are required for RNA selection. These *cis*-acting sequences, called packaging (Psi), or encapsidation, signals, have been identified in avian, murine, and primate retroviruses (13, 14, 17, 19, 23). For Moloney murine leukemia virus (M-MuLV) and human immunodeficiency virus (HIV), packaging signals are located between splice sites and therefore are not contained in the subgenomic mRNAs. The existence of a specific *cis*-acting genomic segment required for high-efficiency RNA encapsidation suggests that it is a recognition site for a *trans*-acting factor, presumably the retroviral Gag protein, since *gag* mutants have been shown to impair RNA encapsidation (1, 10, 18, 24, 27). Gag proteins initially are synthesized as precursor polyproteins which form assembling particles. During or after budding, Pr^{Gag} proteins are cleaved by the viral protease (PR) to yield the mature proteins MA (matrix), p12, CA (capsid), and NC (nucleocapsid) for M-MuLV and MA, CA, NC, and p6 for HIV-1. To date, of these proteins, only mutations in NC have been shown to block encapsidation of viral RNA into virus particles (1, 9, 16, 27). NC deletions and some NC mutations also impair virus assembly (7), suggesting that NC plays a role in virus assembly in addition to viral RNA packaging.

Although some NC mutations can reduce assembly of RNA into virus particles (1, 9), most studies have not addressed how the specificity for encapsidation of the viral genomic RNA is affected. Several in vitro studies have shown that NC binds both specifically and nonspecifically to RNA, so it has been difficult to assess whether mutations affect nonspecific or specific binding to viral genomic RNA (4, 21). One observation which suggests that the NC domain is involved in specific RNA recognition comes from studies of the mutations of the M-MuLV NC Cys-His motif. Several mutations led to the production of noninfectious particles lacking genomic RNA but containing detectable levels of cellular RNA, suggesting an altered binding specificity (10). Similarly, analysis of a chimeric Rous sarcoma virus–M-MuLV Gag protein suggested that some specificity is determined by the NC protein (7). On the basis of the observations mentioned above, we decided to examine the specificity of RNA encapsidation into HIV particles. Examination of an HIV-1 NC Cys-His motif mutant showed that mutant particles encapsidated less viral RNA than wild-type (wt) particles and that the ratio of encapsidated HIV genomic RNA versus spliced RNA was reduced. Additionally, we analyzed a chimeric M-MuLV PR^- Gag protein in which the M-MuLV NC domain was replaced by an HIV-1 NC domain. Our results show that the chimeric protein assembles virus particles and that the wt M-MuLV PR^- Gag protein preferentially encapsidated M-MuLV RNA, while the M-MuLV Gag protein with an HIV NC region preferentially packaged HIV-1 genomic RNA. Our results indicate that at least some of the specificity for encapsidation of HIV RNA is inherent in the NC domain of the Gag protein.

MATERIALS AND METHODS

Recombinant constructs. BlueHX680-831 (27), the recombinant plasmid used to make an antisense riboprobe for detection of HIV RNA, was constructed by using the *Sac*I-*Sal*I fragment from pBluescribe (Stratagene) and an HIV-1 (HXB2) insert (nucleotides [nt] 680 to 83), which was isolated as a *Sac*I-*Sal*I restriction fragment from our HIVgptClaI linker-insertion mutant (27). For

* Corresponding author. Phone: (503) 494-8098. Fax: (503) 494-6862.

detection of M-MuLV transcripts, we used the plasmid SPMLV (2), which contains an M-MuLV *Sac*I-*Bal*I fragment corresponding to proviral nt 420 to 660, inserted into the *Sac*I-*Hin*cII fragment of SP64 (Promega). HIV expression constructs were based on HIVgpt (20, 25, 27), which derives from HXB2 (8). HIVgptA14-15 is a derivative of HIVgpt (25), in which the NC mutations of HIVgptA14-15 (kindly provided by R. Young) were transfered to the HIVgpt backbone. Thus, HIVgptA14-15 has cysteine-to-tyrosine mutations at Gag codons 392, 395, 413, and 416, altering both of the NC Cys-His finger motifs.

pXM2453-wt is a PR-deficient (PR^-) M-MuLV expression vector in which *pol* and *env* genes have been deleted. The M-MuLV sequence starts from the *Pst*I site at viral nt 563, which was altered to *Hin*dIII (19), and ends at the *Nhe*I site at nt 7842 of the M-MuLV viral genome. The internal sequence from the *Bst*EII site at viral nt 2453, which was changed to a *Bam*HI site, to the *Cla*I site at viral nt 7674 (*Cla*I7674) was deleted and replaced by a *Bam*HI-to-*Cla*I fragment derived from a modified pBluescript SK−(Stratagene) polylinker region, in which the pBluescript SK− *Sma*I site was opened and an all-frame *Hpa*I terminator fragment was inserted. The junction sequences between *Bst*EII2453 and *Cla*I7674 are as follows: 5′ CCT AAG GTC ACC GCG GAT CCC CCT **TAA** GTT AAC TTA AGG GCT GCA GGA ATT CGA TAT CAA GCT TAT CGA T 3′, in which the M-MuLV viral nt 2453 (G) and nt 7674 (A) are underlined and the termination codon, TAA, is in boldface type. To facilitate cloning, *Eco*RI adapters were added 5′ to the original *Pst*I site at viral nt 563 (now a *Hin*dIII site) and 3′ of the M-MuLV *Nhe*I site at nt 7842. Thus, the sequence 5′ of nt 563 is 5′ GAATTCGATATCAAGCTT 3′, and the sequence 3′ to nt 7842 is 5′ GCTAGCAGGATCCCCGGGCGACCTCGAATTC 3′, in which the M-MuLV viral nt 7842 (G) is underlined. The *Eco*RI fragment described above was cloned into the *Eco*RI site of pXM (28), an expression vector which uses the adenovirus major late promoter to drive gene expression. The resulting vector, pXM2453-wt, lacks the M-MuLV encapsidation signal (Psi region) and encodes M-MuLV *gag* but not *pol* or *env* genes. The total length of pXM2453-wt is 7,275 bp. Starting from the *Hin*dIII site near the simian virus 40 (SV40) *ori* at nt 0 and upstream of the M-MuLV sequences are the SV40 *ori* (nt 0 to 290), the adenovirus major late promoter and leader (nt 290 to 960), and the adenovirus intron sequences (nt 960 to 1070). Downstream are dihydrofolate reductase RNA stabilization sequences (nt 3215 to 3965), a poly(A) signal (nt 3965 to 4815), and the plasmid backbone (nt 4815 to 7275). Starting from the *Hin*dIII site near the SV40 *ori*, approximate map positions (in nucleotides) for all occurrences of selected enzymes are as follows: *Cla*I, 3023; *Hin*dIII, 0, 960, 1082, 3018; *Eco*RI, 1070, 3006, 3205; *Hpa*I, 2984, 4075; *Xba*I, 4565; *Xho*I, 2079. The vector pXM2453-NCex is the same as pXM2453-wt, except that the NC coding region of M-MuLV was replaced by the HIV-1 NC coding region. This was done by insertion of an HIV-1 NC PCR fragment, with primer-modified ends, in place of the M-MuLV NC fragment from the *Bal*I site at M-MuLV viral nt 2056, to a *Bam*HI site created at nt 2192. The 5′ NC junction sequence is 5′ GCC ACT GTC GTT AGT GGA **ATG CAG AGA GGC** 3′, where HIV nucleotides are in boldface type and M-MuLV nt 2072 (A) and HIV nt 1920 (A) are underlined. The 3′ junction sequence is 5′ **TGT ACT GAG AGA** *GGA TCC CG* T CGG GGA CCA 3′, where HIV sequences again are shown in boldface type, non-M-MuLV and non-HIV linker sequences are shown in italics, and the HIV nt 2075 (A) and M-MuLV nt 2192 (T) are underlined.

Because pXM-based constructs do not possess either M-MuLV or HIV encapsidation signals, it is necessary to supply packageable HIV and M-MuLV transcripts in *trans*. For this purpose, we have employed the vectors HIVGBG831 and B2BAG. HIVGBG831 has the same structure as HIVgpt, except that the *Cla*I831-to-*Sal*I5786 fragment was replaced by the *Escherichia coli* β-galactosidase (β-Gal) gene, in frame, so that HIVGBG831 expresses 15 codons of HIV Gag fused to the ninth codon of β-Gal (26). HIVGBG831 has HIV long terminal repeats, an intact Psi region, and the HIV intron structure, so it produces both spliced and unspliced RNA sequences which can be detected by the HIV probe made from BlueHX680-831. B2BAG is a proviral expression vector, in which the M-MuLV long terminal repeat promoter drives expression of β-Gal and an internal SV40 early promoter with replication origin function (SV40 *ori*) drives expression of a selectable neomycin gene (5). It also has the pBR322 bacterial origin of replication (pBR *ori*) and an M-MuLV Psi region but no splice donors or acceptors.

Cells, viruses, and protein analysis. Cells were grown and transfected as described previously (11, 25–27). Gag proteins in cell lysates and virus particles were detected by immunoblotting (15, 25–27): M-MuLV Gag proteins were detected with a mouse anti-p30 monoclonal antibody (12) as the primary antibody and an alkaline phosphatase-conjugated goat anti-mouse antibody (at 1:1,500) as the secondary antibody, while HIV Gag proteins were detected with an anti-HIV CA monoclonal antibody (Hy183), obtained from Bruce Chesebro through the AIDS Research and Reference Reagent Program. For bis-maleimido hexane (BMH; Pierce) cross-linking of viral Gag proteins, BMH was prepared in dimethyl sulfoxide as a 100 mM solution, and cross-linking followed established protocol (12). For sucrose density gradients, 60-ml supernatants from transfected Cos7 cells were first centrifuged at 4°C for 10 min at 1,000 × *g* to remove cells and debris, after which the cell-free supernatants were centrifuged through 4-ml 20% sucrose cushions in TSE (10 mM Tris-HCl [pH 7.4], 100 mM NaCl, 1 mM EDTA, 0.1 mM phenylmethysulfonyl fluoride) at 4°C for 2 h at 83,000 × *g* (25,000 rpm on an SW28 rotor). The viral pellets were resuspended in 0.5 ml TSE and applied to sucrose gradients consisting of 1.1-ml steps of 20, 30, 40, and 50% sucrose in TSE that had been prepared at least 60 min in advance and placed at 4°C to permit mixing. Gradients were centrifuged at 300,000 × *g* (50,000 rpm on an SW50.1 rotor) overnight at 4°C, and 0.4-ml fractions were collected from top to bottom. The fractions then were mixed and aliquoted for measurement of both sucrose densities and Gag protein levels, which were quantitated from immunoblot bands with a Bio-Rad model 620 densitometer (25).

RNase protections. For RNase protection assays, viral pellets were prepared from 30-ml supernatants of transfected Cos7 cells in the same way as described for the sucrose density gradients. Viral pellets were resuspended in 600 μl of RNase-free Tris-EDTA–sodium dodecyl sulfate (SDS) (50 mM Tris [pH 7.4], 5 mM EDTA, 0.1% SDS), and 0.1-ml aliquots were taken for protein analysis as described above. For viral RNA preparation, 30 μg of *Saccharomyces cerevisiae* tRNA was added to each of the remaining 0.5-ml viral suspensions, and the mixtures were extracted once with phenol-chloroform, once with chloroform, twice with phenol-chloroform, and once with chloroform and then were precipitated with ethanol. The pellets were dried and resuspended in 0.1 ml of 10 mM Tris (pH 7.4)–0.1 mM EDTA. Cellular RNA was isolated from transfected cells as described previously (27), and cellular RNA concentrations were quantitated by measuring the A_{260}, using a Beckman DU-64 spectrophotometer. Riboprobe transcriptions were done with linearized template plasmids according to standard procedures (27). After synthesis, phenol-chloroform extraction, and ethanol precipitation, probe pellets were resuspended in sequence loading dye, heated at 85°C for 5 min, and electrophoresed on a small 5% denaturing polyacrylamide sequencing gel to purify and isolate the probes. Probes excised from gels were eluted by two 30-min incubations at 50°C in 250 μl of 1 M ammonium acetate (pH 7.4)–0.1% SDS–1 mM EDTA, and pooled elutions were combined with 20 μg of yeast tRNA, phenol-chloroform extracted twice, and ethanol precipitated. Dried probe pellets were resuspended in 30 μl of 10 mM Tris (pH 7.4)–0.1 mM EDTA and stored frozen at −80°C for less than 10 days.

For hybridizations with riboprobes, 10% of the viral RNA samples or 40 μg of cellular RNAs was mixed with 10 μg of yeast tRNA, ethanol precipitated, dried, and resuspended for use. Hybridizations, RNase digestions, electrophoresis, and detection have been described previously (27). The HIV probe prepared from BlueHX680-831 is 183 bases in length, including 5′ and 3′ non-HIV sequences derived from the pBluescribe vector. Spliced and unspliced genomic HIV RNAs are expected to yield protected fragments of 63 to 64 bases and 150 bases, respectively. The probe made from SPMLV is 274 bases long, including 5′ and 3′ non-M-MuLV vector sequences. Hybridization of the SP6 transcript to the genomic unspliced M-MuLV RNA should yield a protected fragment of 214 bases after RNase digestion. The protected bands were measured densitometrically. For the RNase and DNase control experiments, equal amounts of viral or cellular RNA were incubated with 0, 30, 100, and 300 μg of RNase or DNase (Boehringer) per ml at 37°C for 1 h. As controls, RNase and DNase solutions (100 μg/ml) also were mock incubated at 37°C for 1 h without adding any RNA. Incubated samples then were mixed with 10 μg of yeast tRNA, phenol-chloroform extracted three times, chloroform extracted twice, and ethanol precipitated. Hybridizations and RNase digestions were carried out as described above, while aliquots of mock-treated samples were processed for electrophoresis directly after hybridization incubations without RNase posttreatment.

RESULTS

RNA encapsidation into wt and NC mutant HIV particles. Previously, we (27) and others (1) observed reduced incorporation of HIV-1 viral RNA into the NC mutant HIVgptA14-15, which substitutes tyrosines for the first two cysteines in each of the NC Cys-His boxes. However, in repeated experiments we observed that the incorporation of viral RNA into the mutant particles was not blocked completely. Because previous experiments suggested that some NC mutations might affect specificity of viral RNA incorporation (1, 27), we examined more closely the specificity of viral RNA encapsidation of the NC Cys-His motif mutant. To do so, Cos7 cells were transfected with wt HIVgpt or NC mutant HIVgptA14-15 constructs, and cellular and viral RNAs were collected. For RNA analysis, we used a 183-base antisense RNA HIV probe which crosses the major splice donor site of HIV-1. Not surprisingly, protection of the HIV probe (Fig. 1A, lane B) was not observed with yeast tRNA (lane A), RNA preparations for mock-transfected Cos7 cells (lane E), or mock media samples (lane H). However, as observed previously, cellular wt or mutant HIVgptA14-15 genomic transcripts protected a fragment of 150 bases while cellular spliced HIV RNAs protected fragments of 63 to 64 bases (Fig. 1, lane C). As shown in Fig. 1A, lane F, wt virus preferentially encapsidated genomic versus spliced viral RNA

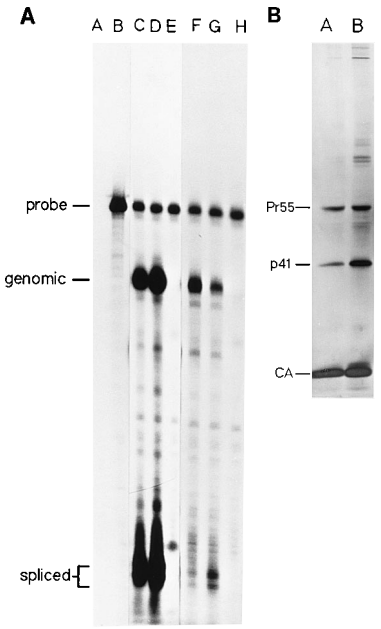

FIG. 1. Encapsidation of HIV RNA into wt and NC mutant particles. (A) Cellular (lanes C through E) and viral (lanes F through H) RNAs were collected from Cos7 cells which were either mock transfected (lanes E and H), or transfected with DNAs encoding wt HIVgpt (lanes C and F) or NC mutant HIVgptA14-15 (lanes D and G). Viral (10% total sample) or cellular (40 μg) RNAs were detected by RNase protection, using the BlueHX680-831 probe as described in Materials and Methods. The probe itself (lane B) is 183 nt long and yields little background with the control yeast tRNA sample (lane A). Since the antisense probe crosses the HIV-1 splice donor, viral genomic transcripts protect a probe fragment of 150 bases, while spliced HIV transcripts protect 63- to 64-base fragments (indicated). (B) For quantitation of Gag protein levels in virus samples from which RNAs were obtained, one-third of the HIVgpt virus samples and one-third of the HIVgptA14-15 virus samples were taken prior to RNA extraction and electrophoresed and immunoblotted with a mouse anti-CA monoclonal primary antibody for HIV Gag protein detection. Lanes A and B are immunoblots of proteins from HIVgpt and HIVgptA14-15 transfections, respectively. The positions of the HIV Gag proteins Pr55, p41, and p24 (CA) are indicated. Note that although minor differences in proteolytic processing were observed, the average ratios of Pr55:p41:CA were 20:24:56 (29 transfections) for HIVgpt and 17:28:55 (11 transfections) for HIVgptA14-15.

(compare lanes F and C), while HIVgptA14-15 virions packaged genomic and spliced RNAs at roughly equal levels (lane G). Because the amount of Gag protein in virus samples was slightly higher for HIVgptA14-15 than for HIVgpt (Fig. 1B), it appears that HIVgptA14-15 reduced both the specificity of viral RNA packaging (as determined by the reduced ratio of genomic RNA versus spliced RNA [23]) and the amount of viral RNA encapsidated (as determined by the ratio of viral RNA to Gag protein).

In order to quantitate our results, viral Gag protein levels and cellular and viral RNA levels were quantitated densitometrically to obtain the results shown in Table 1. As shown, the HIVgpt viral genomic RNA signal was higher than that of HIVgptA14-15, and the ratio of the viral genomic RNA signal to viral Gag protein levels was higher for HIVgpt than for HIVgptA14-15. However, the difference between wt and mutant genomic RNA-to-Gag ratios was three- to fourfold, suggesting that an intact NC Cys-His motif is not absolutely essential for incorporation of RNA into virus particles. In terms of specificity, the ratio of viral genomic RNA to spliced RNA of HIVgpt was ninefold higher than that of HIVgptA14-15 done in parallel (Table 1). Since the levels of genomic and spliced RNAs in virus samples were determined at the same time in the same samples and viral versus cellular genomic RNA/spliced RNA ratios were 10-fold higher for wt than for mutant virus (Table 1), the observed specificity differences in virus particles appeared independent of potential sample differences or major differences in cellular RNA levels.

Although these results showed that the Cys-His mutant (HIVgptA14-15) affected levels and specificity of encapsidation, the effect was not as great as one might have predicted, given the observation that wt HIV is over 1,000-fold more infectious than such NC mutants (10, 25, 27). Since this could have been due to some unusual feature of the Cos7-SV40 expression system, we repeated our experiments with HeLa cells and obtained similar results (data not shown). A separate concern was that the apparent viral genomic RNA signals in our cell or virus samples could have been due to contamination of RNA samples with transfected DNA. To control for this possibility, viral and cellular RNA samples were pretreated with either DNase or RNase before phenol-chloroform extraction, ethanol precipitation, and hybridizations. As shown in Fig. 2, DNase treatment of viral (lanes L through N) or cellular (lanes D through F) RNA samples did not affect signal detections relative to mock-treated controls (lanes G and O). In contrast, RNase pretreatment (Fig. 2, lanes H through J and P through R) eliminated RNase protection signals relative to mock-treated controls (lanes K and S). Since sample pretreatment with either DNase (Fig. 2, lane B) or RNase (Fig. 2, lane C) did not cause probe degradation, these results indicate that the protected fragments are due to signals from viral and cellular RNAs and not to signals from transfected DNA.

RNA encapsidation into chimeric virus particles. Because the HIV NC mutant HIVgptA14-15 appeared to lose some degree of viral genomic RNA packaging specificity, we attempted the complementary experiment, to see if increased encapsidation specificity could be transferred to another virus with the HIV NC domain. To do so, we chose to make a chimera of the M-MuLV Gag MA, p12, and CA domains with the HIV-1 NC domain, which would allow us to test NC effects on encapsidation. The parental construct, pXM2453-wt (Fig. 3), expresses the M-MuLV Gag protein from the adenovirus major late promoter and deletes almost all of the *pol* gene, to eliminate potential difficulties of Gag and Gag-Pol interactions. The construct also lacked the M-MuLV Psi signal, so it would be possible to provide HIV or M-MuLV packageable

TABLE 1. RNA encapsidation in wt and NC mutant HIV particles[a]

Virus	Viral G RNA level[b]	Viral G RNA/ cell G RNA	Viral G RNA/ viral S RNA	(Viral G/S RNA)/ (cell G/S RNA)	Viral G RNA/ viral Gag protein
wt	1,750	0.54	5.81	7.85	0.57
HIVgptA14-15	694	0.17	0.62	0.76	0.15

[a] Cellular and viral RNAs were detected and Gag protein levels were monitored as described in the legend to Fig. 1. RNase protection bands and Gag immunoblot bands from Fig. 1 were densitometrically quantitated, using a Bio-Rad model 620 scanning densitometer. Note that in five separate transfections, HIVgpt viral genomic RNA/spliced RNA ratios were 2.7- to 9.4-fold higher than HIVgptA14-15 ratios. G, genomic; S, spliced.

[b] The values listed are arbitrary densitometer units.

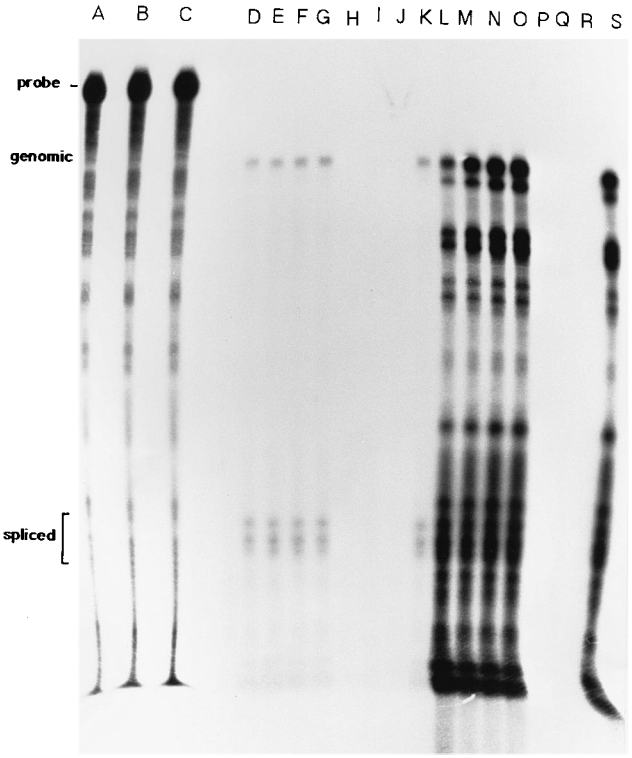

FIG. 2. RNase protection controls. To demonstrate that probe protection was from sample RNA rather than transfected plasmid DNAs, equal amounts of HIV viral RNA (lanes L through S) and equal amounts of HIVgpt-transfected Cos7 cellular RNA (lanes D through K) were incubated for 1 h at 37°C in 300, 100, 30, and 0 μg of RNase per ml (lanes H through K and lanes P through S, respectively) or DNase (lanes L through O and lanes D through G, respectively). RNase and DNase solutions also were incubated at 37°C without adding any RNA (lanes C and B). After incubations, the samples were mixed with 10 μg of yeast tRNA, phenol-chloroform extracted three times, chloroform extracted twice, and ethanol precipitated. Hybridizations and RNase digestion were carried out as described in Materials and Methods. For lanes C and B, RNase digestions was not performed after hybridization, but aliquots of the hybridization mixtures were loaded directly onto the gel instead. The positions of the probe (lane A) and of the unspliced and spliced HIV RNAs are indicated. Note that these results were obtained in three separate experiments and that input DNA came from pooled stocks of cellular and viral DNA, so that ratios of cellular versus viral RNA levels are not meaningful here.

RNAs separately. To substitute the HIV NC domain for the M-MuLV NC domain in pXM2453-wt, the HIV-1 NC coding region (excluding the three carboxy-terminal codons) was inserted in place of the central 40 codons of M-MuLV NC. The resulting chimeric construct, pXM2453-NCex, has M-MuLV MA, p12, and CA and the first six residues of M-MuLV NC, 52 of the 55 codons of HIV-1 NC, a linker containing three foreign residues (GSD), and the last 14 codons of M-MuLV NC (Fig. 3).

Since NC has been implicated in retrovirus assembly, one concern about our chimeric construct pXM2453-NCex was that it might not produce virus particles or that the particles produced might not be like wt viruses. The first step in the analysis of whether our chimeric protein could produce virus particles was to determine whether the chimeric Gag proteins were released from transfected cells. To do so, plates of Cos7 cells were transfected with pXM2453-wt or pXM2453-NCex, and Gag proteins in cell lysates and virus particles were examined by immunoblotting (Fig. 4). A comparison of the ratios of cellular versus viral Gag protein levels for pXM2453-wt (Fig. 4, lanes A and B) and pXM2453-NCex (lanes D and E) showed that chimeric Gag proteins were released at levels equal to those of the wt M-MuLV Pr^{Gag} proteins. To test whether chimeric Gag proteins formed virus particles that were structurally similar to wt viruses, we next tested the densities of the chimeric and wt viruses. Supernatants from Cos7 cells transfected with pXM2453-wt or pXM2453-NCex were collected, pelleted, resuspended, mixed with internal-control wt HIV virus, and fractionated by sucrose density gradient centrifugation (10 to 50%). Aliquots of fractions were collected to measure sucrose densities and levels of both M-MuLV and HIV Gag proteins. As shown in the top panel of Fig. 5, virus particles formed by wt M-MuLV Pr^{Gag} proteins expressed by pXM2453-wt had a density of 1.15 g/ml, while the internal control (HIV; thin line) had a slightly lower density of 1.14 g/ml. This result is consistent with the slightly different densities observed for different retroviruses by others (3). As shown in the bottom panel of Fig. 5, virus particles assembled from the chimeric Gag protein expressed by pXM2453-NCex had the same density as wt M-MuLV, again slightly higher than that of HIV (thin line). To further validate the structural similarity between the chimeric virus and wt M-MuLV, we tested

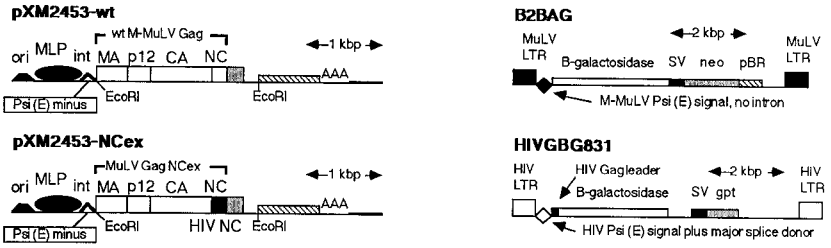

FIG. 3. Recombinant viral constructs. pXM2453-wt is an expression vector which uses the adenovirus major late promoter (MLP; black oval) to drive the expression of the M-MuLV *gag* gene. The encapsidation signal and *pol* and *env* genes of the M-MuLV sequences were deleted, and the M-MuLV coding region terminates at the protease region (grey box). Other features of this construct are the adenovirus leader and intron (int), 3′ noncoding dihydrofolate reductase sequences (striped box), and the poly(A) signal. SV40 *ori* and ColE1 *ori* permit plasmid replication in both Cos7 cells and bacteria. Shown is the 4,815-bp M-MuLV *gag* gene expression unit and not the pUC12 plasmid backbone. The *Eco*RI sites are at nt 1070 and 3205, and occurrences of other selected restriction endonuclease sites are noted in Materials and Methods. pXM2453-NCex is similar to pXM2453-wt, except that the M-MuLV NC coding region was replaced by the HIV-1 NC coding region as described in Materials and Methods. Consequently, pXM2453-NCex encodes a *gag* fusion gene, retaining M-MuLV *gag* MA, p12, and CA domains fused to a C-terminal HIV NC domain. Because neither pXM2453-wt or pXM2453-NCex retains a packaging signal, we have used B2BAG and HIVGBG831 in encapsidation studies. B2BAG is a retroviral expression vector and is shown in its proviral form. The M-MuLV long terminal repeat (LTR) promoter drives expression of the *E. coli* β-Gal gene, and an internal SV40 early promoter, which also retains replication origin capabilities (SV *ori*), drives the expression of the selectable neomycin (*neo*) gene. The M-MuLV encapsidation signal (black diamond) is intact, but splice signals have been removed. HIVGBG831, shown in its proviral form, is similar to B2BAG in that it expresses both β-Gal and a second gene (*gpt*) from an internal SV40 promoter. The HIVGBG831 β-Gal gene is driven by the HIV-1 long terminal repeat promoter and retains 15 amino-terminal codons from the HIV *gag* MA domain. HIVGBG831 also retains the HIV-1 leader and encapsidation signal region (white diamond) and expresses a genomic transcript, as well as spliced messages which lack the encapsidation signal.

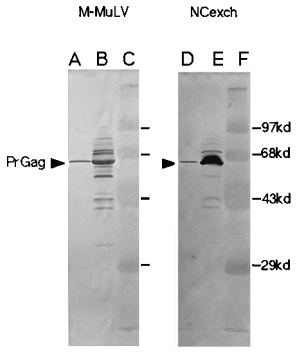

FIG. 4. Release of M-MuLV and NC exchange Gag proteins from transfected cells. Twenty micrograms each of pXM2453-wt or pXM2453-NCex was transfected onto separate plates of Cos7 cells. Three days posttransfection, supernatants and cells were collected and prepared for SDS-PAGE as described in Materials and Methods. Supernatant samples (lane B, pXM2453-wt; lane E, pXM2453-NCex) and cell samples (lane A, pXM2453-wt; lane D, pXM2453-NCex) were electrophoresed and electroblotted onto a nitrocellulose filter. M-MuLV Gag proteins were detected by immunoblotting with a mouse anti-M-MuLV CA monoclonal antibody as the primary antibody and a secondary alkaline phosphatase-conjugated goat anti-mouse antibody at a 1:1,500 dilution. Size standards are in lanes C and F, molecular masses are indicated on the right, and the M-MuLV Pr^{Gag} proteins are indicated by arrowheads.

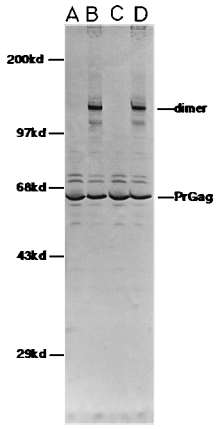

FIG. 6. Cross-linking of Gag proteins in viruses. Virus pellets prepared from supernatants of Cos7 cells transfected with pXM2453-wt (lanes A and B) or pXM2453-NCex (lanes C and D) were resuspended in 200 μl of TSE and split into equivalent 100-μl fractions that were mock treated (lanes A and C) or cross-linked at cysteines with BMH (lanes B and D). After treatment, the samples were electrophoresed and immunoblotted for detection of Gag proteins, as described in Materials and Methods. Molecular mass marker sizes are shown on the left, while Pr^{Gag} monomers and dimers are indicated on the right.

the abilities of Pr^{Gag} proteins in chimeric and wt virus particles to be cross-linked by BMH. Previous studies showed that Pr^{Gag} NC cysteine residues in intact M-MuLV and HIV particles can be cross-linked with either iodine or BMH to yield Gag protein dimers (12), demonstrating that NC domains in immature viruses are in close proximity to each other. To test chimeric and wt M-MuLV viruses, pelleted particles were mock treated or BMH cross-linked, after which Gag proteins were separated by SDS-polyacrylamide gel electrophoresis (PAGE) and detected by immunoblotting. As expected, Pr^{Gag} proteins in wt virions cross-linked via cysteines to form dimers when BMH treated (Fig. 6, lane B), while dimer formation was not observed for the parallel mock-treated sample (lane A). We also observed that Pr^{Gag} proteins in chimeric particles cross-linked via Gag cysteines (Fig. 6, compare lanes D and C). These experiments suggest that the chimeric virus particles produced from pXM2453-NCex are similar to wt M-MuLV viruses, at least at this level of biochemical analysis.

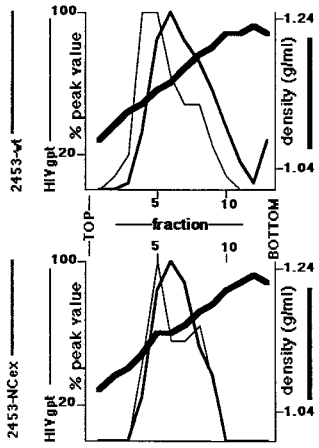

FIG. 5. Density gradient fractionation of wt and NC exchange viruses. Six plates of Cos7 cells were transfected with either pXM2453-wt or pXM2453-NCex. Three days posttransfection, media supernatants were collected and viral pellets were prepared as described in Materials and Methods. The pellets were resuspended in 0.5 ml of TSE mixed with an internal-control HIV (HIVgpt) virus stock and fractionated on sucrose density gradients (10 to 50%). Fractions, shown on the *x* axis, were collected from top to bottom, and aliquots were used to measure sucrose densities and HIV and M-MuLV Gag protein levels. The thick black line indicates gradient densities in grams per milliliter, as indicated on the right-hand *y* axis. Internal-control HIV Gag protein levels, shown as percentages of the peak fraction value for a gradient, are indicated by thin black lines, and pXM2453-wt (top panel) or pXM2453-NCex protein levels (bottom panel) are indicated by intermediate black lines.

With our assembly-competent chimeric virus, it was possible to test whether encapsidation specificity could be transferred with the HIV NC domain. Since the transcripts from pXM2453-wt and pXM2453-NCex do not possess the Psi signals, they cannot be packaged into the virus particles produced by these constructs. However, this feature has allowed us to provide potentially packageable transcripts from other constructs in *trans* and to evaluate encapsidation efficiencies. The packageable M-MuLV vector was B2BAG (3) (Fig. 3), which expresses a viral genomic transcript retaining the M-MuLV encapsidation signal and encoding β-Gal. For HIV, we employed HIVGBG831 (6) (Fig. 3), which encodes an HIV Gag–β-Gal fusion protein that has only 15 residues of HIV Gag, produces both viral genomic and spliced transcripts, and retains the putative HIV encapsidation signal on its genomic RNA. To examine encapsidation, Cos7 cells were transfected with pXM2453-wt or pXM2453-NCex plus either B2BAG or HIVGBG831. At 72 h posttransfection, viral protein samples and cellular and viral RNA samples were collected and processed for analysis. As shown in Fig. 7A, when pXM2453-wt and pXM2453-NCex were cotransfected with B2BAG, the detected cellular levels of the B2BAG message were approximately equal (Fig. 7A, lanes C and D). In contrast, viruses produced from pXM2453-wt showed higher B2BAG RNA levels than did viruses made from pXM2453-NCex (Fig. 7A, compare lanes A and B). Since the amount of Pr^{Gag} protein in the pXM2453-wt virus sample was equal to or less than that of pXM2453-NCex (Fig. 7C, compare lanes A and B), these results suggest that the specificity of wt M-MuLV Pr^{Gag} is greater than that of the chimeric Pr^{Gag} protein for the M-MuLV B2BAG transcript. The reverse was true when pXM2453-wt and pXM2453-NCex were cotransfected with HIVGBG831. While HIVGBG831 genomic and spliced RNAs were detected

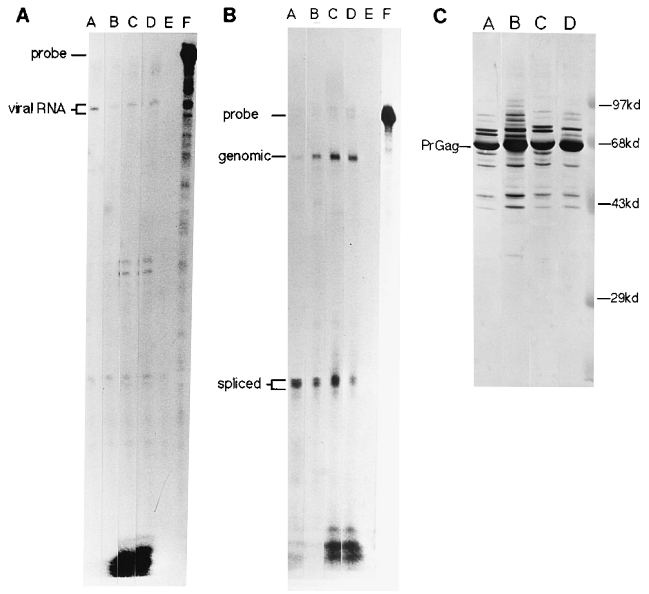

FIG. 7. RNA incorporation into M-MuLV and NC exchange viruses. Plasmid pXM2453-wt or pXM2453-NCex was cotransfected with either B2BAG or HIVGBG831 onto Cos7 cells, using six plates of cells for each cotransfection. Viruses were pelleted from media supernatants, and an aliquot was used for Gag protein detection. In parallel, virus RNAs were prepared, and RNase protection assays were performed as described in Materials and Methods. (A) The SPMLV probe was used as described in Materials and Methods to detect B2BAG RNA in virus (lanes A and B) and cell (lanes C and D) samples from cells transfected with pXM2453-wt plus B2BAG (lanes A and C) or pXM2453-NCex plus B2BAG (lanes B and D). The probe band (lane F) is indicated, as is the fragment protected by the B2BAG genomic message. In lane E, yeast tRNA was used as a negative control. (B) The BlueHX680-831 probe was used as described in the legend to Fig. 1 to detect HIVGBG831 genomic and spliced RNAs in virus (lanes A and B) and cell (lanes B and D) samples of cells transfected with pXM2453-wt plus HIVGBG831 (lanes A and C) or pXM2453-NCex plus HIVGBG831 (lanes B and D). Lane F contained probe alone, and lane E derived from a negative control yeast tRNA sample. The HIVGBG831 genomic and spliced RNA protection fragments are indicated. (C) Aliquots of the virus samples used for RNase protections were subjected to SDS-PAGE and immunoblot detection of Gag proteins for control quantitation purposes. Proteins correspond to the cotransfections described for panels A and B as follows: lane A, pXM2453-wt plus B2BAG; lane B, pXM2453-NCex plus B2BAG; lane C, pXM2453-wt plus HIVGBG831; lane D, pXM2453-NCex plus HIVGBG831. Protein standard marker sizes are shown on the right, and Pr^{Gag} bands are indicated on the left.

at approximately equal levels in cell samples (Fig. 7B, lanes C and D), when viral RNAs were detected with the HIV probe prepared from BlueHX680-831 we found that the viruses produced from pXM2453-wt packaged spliced RNA but very little HIV genomic RNA (Fig. 7B, lane A). In contrast, the viruses produced from pXM2453-NCex showed more particle-associated HIV genomic RNA (Fig. 7B, lane B), and the ratio of genomic to spliced HIV RNA in these particles was higher than that of the viruses produced from pXM2453-wt. Again, because the levels of Gag proteins in the viral samples were approximately equal (Fig. 7C, lanes C and D), these data suggest that retrovirus NC domains provide some specificity toward the recognition of viral transcripts.

To quantitate our results, RNA and Gag protein levels were quantitated densitometrically to obtain the data shown in Table 2. As shown, the raw signal of viral genomic RNA was higher for B2BAG with pXM2453-wt than with pXM2453-NCex and higher for HIVGBG831 with pXM2453-NCex than with pXM2453-wt. Similar results were obtained when genomic RNA levels were normalized for total Gag protein levels. Also, the ratio of viral to cellular B2BAG RNA of pXM2453-wt was higher than that of pXM2453-NCex, and the reverse was true when the ratio of viral to cellular genomic HIVGBG831 transcript was considered. Furthermore, the specificity of HIVGBG831 RNA packaging, which could be monitored by measuring ratios of genomic versus spliced RNAs in single hybridization reactions, showed that particles produced from pXM2453-NCex encapsidated genomic HIV RNA with a specificity ratio (genomic versus spliced) that was fourfold higher than that of the viruses produced from pXM2453-wt. Taken together, these experiments show that the HIV NC domain contributes toward the specificity of RNA encapsidation and that this contribution can act independently of the natural Pr^{Gag} context and *pol* or *env* gene products.

DISCUSSION

Retroviral genomic RNA is packaged preferentially into the virus particles over a high background of cellular RNAs and spliced viral messages. This appears to be achieved by an interaction between the Psi packaging (encapsidation) signal on the viral genomic RNA and the viral Gag proteins, but the precise nature of the interaction is unknown. The results of our study confirm that mutations in the Cys-His motif of HIV NC reduce the total quantity of viral genomic RNA packaged into the particles, as we and others have observed before (1, 10, 27). However, the zinc finger motif mutations in the construct HIVgptA14-15 did not eliminate encapsidation of viral RNA completely, and a comparison of genomic versus spliced RNA levels in mutant NC particles produced showed that the specificity of viral genomic RNA encapsidation was reduced (Fig. 1 and Table 1). These results imply that the HIV NC domain is not just a nonspecific RNA-binding moiety but also provides at least some specificity to RNA encapsidation, which is in agreement with several previous studies (4, 6, 7, 22).

One implication of our result with the NC Cys-His motif mutant was that encapsidation specificity might be transferred to another virus with the HIV NC domain. Thus, we exchanged the M-MuLV NC domain for HIV NC, making a chimera of M-MuLV Gag MA, p12, and CA domains with the HIV NC

TABLE 2. HIV NC effects on RNA encapsidation into M-MuLV particles[a]

Virus	Viral G RNA level[b]	Viral G RNA/ cell G RNA	Viral G RNA/ viral S RNA	(Viral G/S RNA)/ (cell G/S RNA)	Viral G RNA/ viral Gag protein
pXM2453-wt + B2BAG	1,337	2.45			0.34
pXM2453-NCex + B2BAG	312	0.55			0.06
pXM2453-wt + HIVGBG831	85	0.15	0.14	0.20	0.03
pXM2453-NCex + HIVGBG831	265	0.60	0.54	0.44	0.06

[a] Protein and RNA levels were quantitated from immunoblots and RNase protection gels by densitometry. Note that genomic RNA/spliced RNA ratios and double ratios are not provided for B2BAG cotransfections, since B2BAG does not encode a spliced message. G, genomic; spliced, S.

[b] The values listed are arbitrary densitometer units.

domain. Although we previously observed that M-MuLV NC deletion mutants do not assemble virus particles (12), the chimeric Pr^{Gag} protein produced from pXM2453-NCex directed the assembly of particles (Fig. 4 to 6). In encapsidation studies, we found that, in an M-MuLV context, M-MuLV NC contributed to some specificity for M-MuLV transcripts, and HIV NC contributed to specificity for HIV transcripts (Fig. 7 and Table 2). These results are in agreement with those of Dupraz and Spahr (7), who showed that chimeric Gag proteins containing the Rous sarcoma virus NC domain in place of M-MuLV NC showed an increased specificity to packageable Rous sarcoma virus transcripts. Taken together, these results suggest that retroviral NC domains contribute toward the specificity of encapsidation. Furthermore, this level of specificity is not dependent on *pol* gene products, since *pol* is deleted in pXM2453-wt and pXM2453-NCex. However, in our experiments with HIV NC mutants and exchanges (Fig. 1 and 7 and Tables 1 and 2), the maximum encapsidation differences observed were only about 10-fold. Consequently, it seems likely that other regions in Gag or Gag-Pol may add to encapsidation specificity. For instance, NC may interact with another Gag or Gag-Pol domain to allow more efficient recognition of the genomic packaging signal and drive viral genomic RNA encapsidation specificity. Such possibilities are currently under investigation.

ACKNOWLEDGMENTS

We are grateful to Chin-Tien Wang, Mark Hansen, Marylene Mougel, Lori Farrell, Jenny Stegeman-Olsen, and Jason McDermott for assistance and advice throughout the course of this work. The anti-M-MuLV-CA monoclonal antibody was a gift from Bruce Chesebro, who also made the anti-HIV CA Hy183 hybridoma cell line that was obtained from the AIDS Research and Reference Reagent Program, Division of AIDS, NIAID, NIH.

This work was supported by a grant from the National Institutes of Health (NCI grant 5R01 CA 47088-07).

REFERENCES

1. **Aldovini, A., and R. A. Young.** 1990. Mutations of RNA and protein sequences involved in human immunodeficiency virus type 1 packaging result in production of noninfectious virus. J. Virol. **64:**1920–1926.
2. **Barklis, E., R. C. Mulligan, and R. Jaenisch.** 1986. Chromosomal position or virus mutation permits retrovirus expression in embryonal carcinoma cells. Cell **47:**391–399.
3. **Bennett, R. P., T. D. Nelle, and J. W. Wills.** 1993. Functional chimeras of the Rous sarcoma virus and human immunodeficiency virus Gag proteins. J. Virol. **67:**6487–6498.
4. **Berkowitz, R. D., J. Luban, and S. P. Goff.** 1993. Specific binding of human immunodeficiency virus type 1 *gag* polyprotein and nucleocapsid protein to viral RNAs detected by RNA mobility shift assays. J. Virol. **67:**7190–7200.
5. **Berwin, B., and E. Barklis.** 1993. Retrovirus-mediated insertion of expressed and nonexpressed genes at identical chromosomal locations. Nucleic Acids Res. **21:**2399–2407.
6. **Dannull, J., A. Surovoy, G. Jung, and K. Moelling.** Specific binding of HIV-1 nucleocapsid protein to PSI RNA in vitro requires N-terminal zinc finger and flanking basic amino acid residues. EMBO J. **13:**1523–1533.
7. **Dupraz, P., and P. F. Spahr.** 1992. Specificity of Rous sarcoma virus nucleocapsid protein in genomic RNA packaging. J. Virol. **66:**4662–4670.
8. **Fisher, A. G., M. B. Feinberg, S. F. Josephs, M. E. Harper, L. M. Marselle, G. Reyes, F. A. Gonda, A. Aldovini, C. Debouk, R. C. Gallo, and F. Wong-Staal.** 1986. The transactivator gene of HTLV-III is essential for virus replication. Nature (London) **320:**367–371.
9. **Gorelick, R. J., S. M. Nigida, Jr., J. W. Bess, Jr., L. O. Arthur, L. E. Henderson, and A. Rein.** 1990. Noninfectious human immunodeficiency virus type 1 mutants deficient in genomic RNA. J. Virol. **64:**3207–3211.
10. **Gorelick, R. J., L. E. Henderson, J. P. Hanser, and A. Rein.** 1988. Point mutants of Moloney murine leukemia virus that fail to package viral RNA: evidence for specific RNA recognition by a "zinc finger-like" protein sequence. Proc. Natl. Acad. Sci. USA **85:**8420–8424.
11. **Graham, R., and A. van der Eb.** 1973. A new technique for the assay of infectivity of human adenovirus 5 DNA. Virology **52:**456–467.
12. **Hansen, M. S. T., and E. Barklis.** 1995. Structural interactions between retroviral Gag proteins examined by cysteine cross-linking. J. Virol. **69:**1150–1159.
13. **Katz, R. A., R. W. Terry, and A. M. Skalka.** 1986. A conserved *cis*-acting sequence in the 5′ leader of avian sarcoma virus RNA is required for packaging. J. Virol. **59:**163–167.
14. **Koyama, T., F. Harada, and S. Kawai.** 1984. Characterization of a Rous sarcoma virus mutant defective in packaging its own genomic RNA: biochemical properties of mutant TK15 and mutant-induced transformants. J. Virol. **51:**154–162.
15. **Laemmli, U. K.** 1970. Cleavage of structural proteins during the assembly of the head of bacteriophage T4. Nature (London) **227:**680–685.
16. **Lee, P. P., and M. L. Linial.** 1994. Efficient particle formation can occur if the matrix domain of human immunodeficiency virus type 1 Gag is substituted by a myristylation signal. J. Virol. **68:**6644–6654.
17. **Lever, A., H. Gottlinger, W. Haseltine, and J. Sodroski.** 1989. Identification of a sequence required for efficient packaging of human immunodeficiency virus type 1 RNA into virions. J. Virol. **63:**4085–4087.
18. **Linial, M., E. Medeiros, and W. S. Hayward.** 1978. An avian oncovirus mutant (SE21Q1b) deficient in genomic RNA: biological and biochemical characterization. Cell **15:**1371–1381.
19. **Mann, R., R. C. Mulligan, and D. Baltimore.** 1983. Construction of a retrovirus packaging mutant and its use to produce helper-free defective retrovirus. Cell **33:**153–159.
20. **Page, K. A., N. R. Landau, and D. R. Littman.** 1990. Construction and use of a human immunodeficiency virus vector for analysis of virus infectivity. J. Virol. **64:**5270–5276.
21. **Prats, A. C., L. Sarih, C. Gabus, S. Litvak, G. Keith, and J. L. Darlix.** 1988. Small finger protein of avian and murine retroviruses has nucleic acid annealing activity and positions the replication primer tRNA onto genomic RNA. EMBO J. **7:**1777–1783.
22. **Sakaguchi, K., N. Zambrano, E. T. Baldwin, B. A. Shapiro, J. W. Erickson, J. G. Omichinski, G. M. Clore, A. M. Gronenborn, and E. Appella.** 1993. Identification of a binding site for the human immunodeficiency virus type 1 nucleocapsid protein. Proc. Natl. Acad. Sci. USA **90:**5219–5223.
23. **Sakalian, M., J. Wills, and V. M. Vogt.** 1994. Efficiency and selectivity of RNA packaging by Rous sarcoma virus Gag deletion mutants. J. Virol. **68:**5969–5981.
24. **Shank, P. R., and M. Linial.** 1980. Avian oncovirus mutant (SE21Q1b) deficient in genomic RNA: characterization of a deletion in the provirus. J. Virol. **36:**450–456.
25. **Wang, C.-T., and E. Barklis.** 1993. Assembly, processing, and infectivity of human immunodeficiency virus type 1 Gag mutants. J. Virol. **67:**4264–4273.
26. **Wang, C. T., J. Stegeman-Olsen, Y. Zhang, and E. Barklis.** 1994. Assembly of HIV Gag-β-galactosidase fusion proteins into virus particles. Virology **200:**524–534.
27. **Wang, C.-T., Y. Zhang, J. McDermott, and E. Barklis.** 1993. Conditional infectivity of a human immunodeficiency virus matrix domain deletion mutant. J. Virol. **67:**7067–7076.
28. **Yang, Y.-C., A. B. Ciarletta, P. A. Temple, R. P. Chung, S. Kovacic, J. S. Witek-Giannotti, A. C. Leary, R. Kriz, and S. C. Clark.** 1986. Human IL-3 (multi-CSF): identification by expression cloning of a novel hematopoietic growth factor related to murine IL-3. Cell **47:**3–10.